Supporting Information for:

Ultrafast Photoluminescence Kinetics from Hot Excitonic States in CdSe Nanocrystals

*Rafael López-Arteaga, Jorge Peon**

Instituto de Química, Universidad Nacional Autónoma de México, Circuito Exterior, Ciudad Universitaria, Ciudad de México, 04510, México

AUTHOR INFORMATION

Corresponding Author

*e-mail jpeon@unam.mx

Contents:

Table S1. Deconvolution absorption spectrum parameters obtained for D = 4.4 nm quantum dots. $r^2 = 0.99$, the cubic baseline function was $y = (3.63) + (-0.0163)x + (2.47E\text{-}05)x^2 + (-1.25E\text{-}08)x^3$.

State	Amplitude [Absorbance]	Center [nm]	fwhm [nm]	Asym50
X_5	0.032	439	52	0.77
X_4	0.052	483	45	0.70
$X_3(1P_{3/2}1P)$	0.061	514	41	0.96
$X_2(2S_{3/2}1S)$	0.046	566	31	0.67
$X_1(1S_{3/2}1S)$	0.091	595	27	0.87

Table S2. Deconvolution absorption spectrum parameters obtained for D = 5.4 nm quantum dots. $r^2 = 0.99$, the cubic baseline function was $y = (2.58) + (-0.0093)x + (1.09E\text{-}05)x^2 + (-4.07E\text{-}09)x^3$.

State	Amplitude [Absorbance]	Center [nm]	fwhm [nm]	Asym50
X_6	0.026	442	28	0.84
X_5	0.030	477	34	0.85
X_4	0.056	511	30	0.91
$X_3(1P_{3/2}1P)$	0.053	543	30	1.23
$X_2(2S_{3/2}1S)$	0.045	593	24	0.99
$X_1(1S_{3/2}1S)$	0.081	619	24	1.02

Table S3. Fit parameters for the photoluminescence histograms of D = 4.4 nm quantum dots.

Exponential	I / [kCnts]	τ / ns
1	1870 ± 120	60 ± 2
2	2560 ± 210	21 ± 0.9
3	250 ± 40	2.7 ± 0.4

Table S4. Fit parameters for the photoluminescence histograms of D = 5.4 nm quantum dots.

Exponential	I / [kCnts]	τ / ns
1	990 ± 80	67 ± 3
2	2920 ± 40	23 ± 1
3	450 ± 50	4.1 ± 0.6

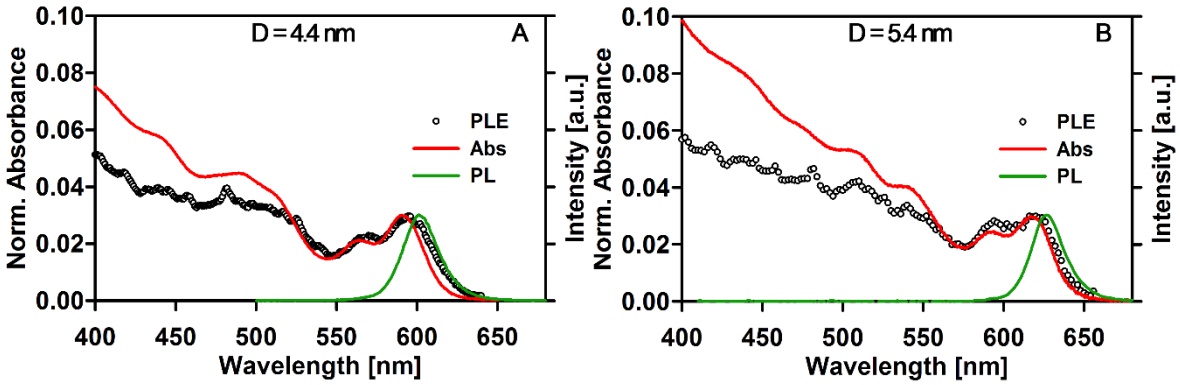

Figure S1. Absorption, emission and photoluminescence excitation spectra of D = 4.4 (A) and 5.4 (B) nm quantum dots.

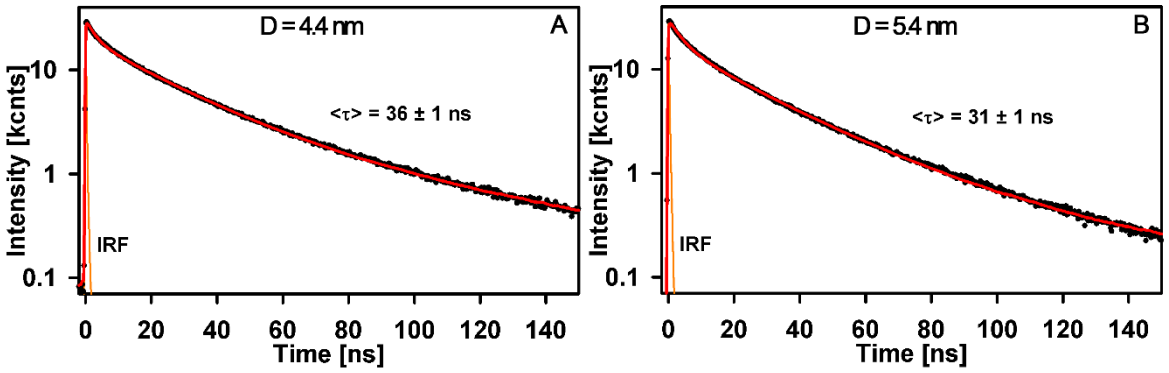

Figure S2. Photoluminescence decay histograms for D = 4.4 (A) and 5.4 (B) nm CdSe quantum dots.

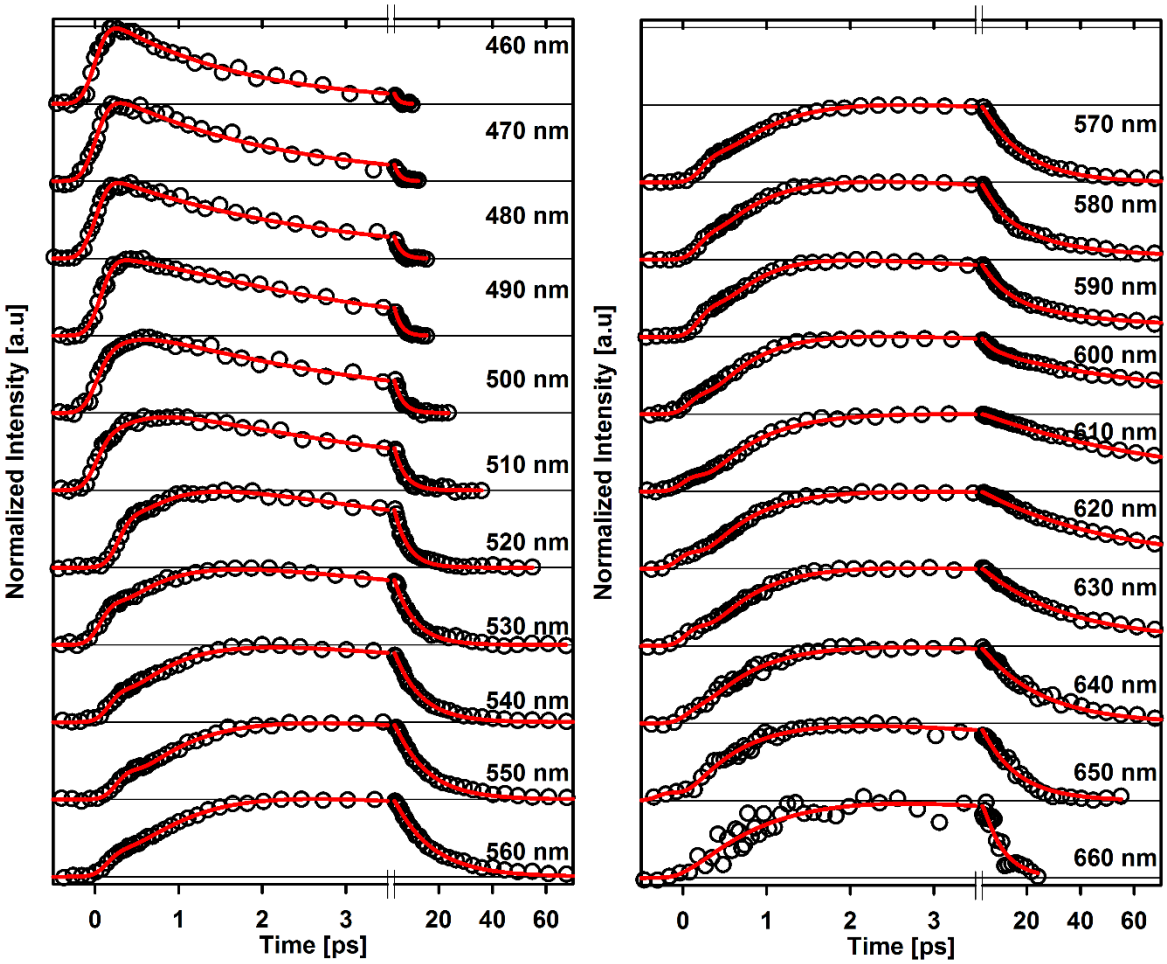

Figure S3. Photoluminescence up-conversion transients for D = 4.4 nm quantum dots detected at the indicated wavelengths.

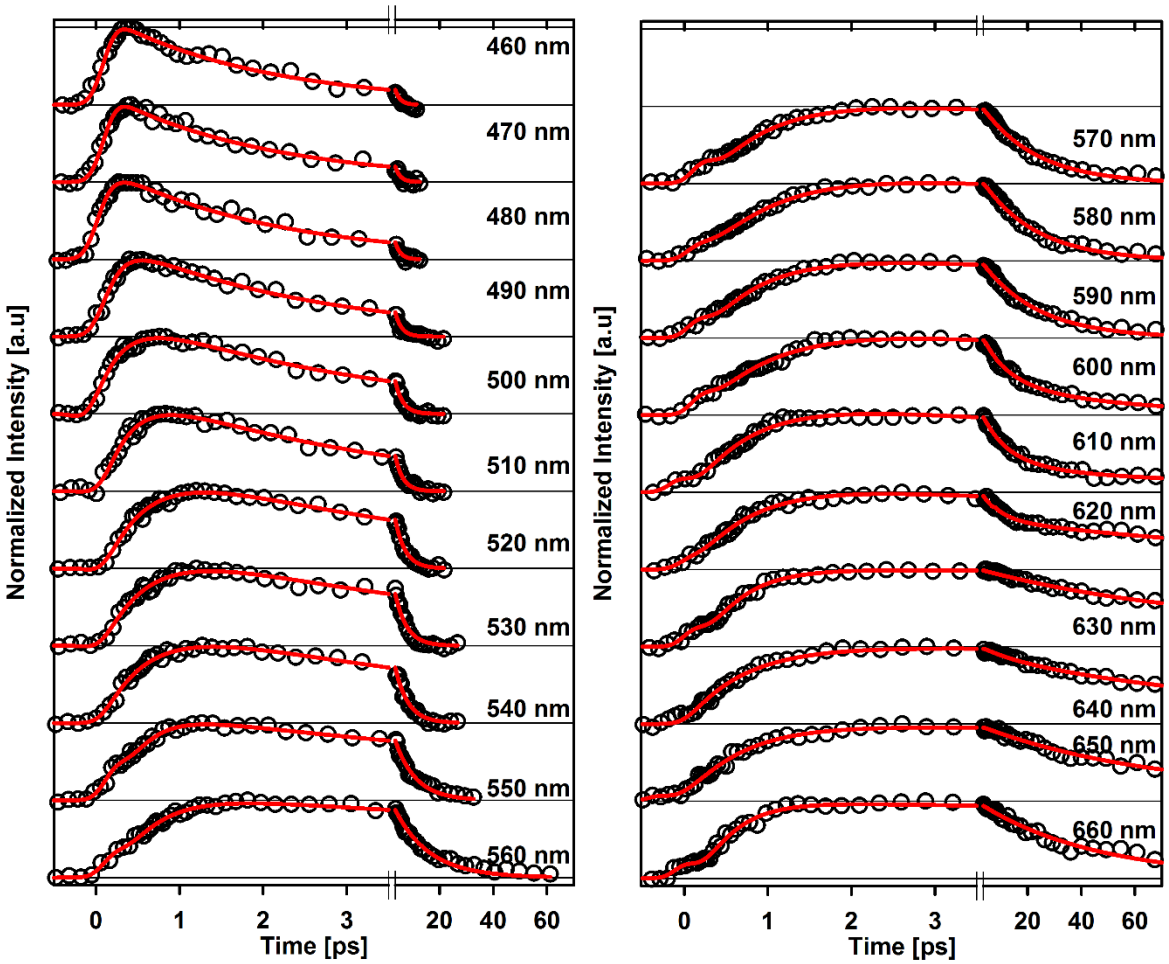

Figure S4. Photoluminescence up-conversion transients for D = 5.4 nm quantum dots detected at the indicated wavelengths.

Table S5. Complete set of fit parameters for D = 4.4 nm quantum dots PL up-conversion signals detected at different wavelengths. Notice the negative sign for the first and second terms.

State	λ/nm	(-)%	τ_1/ps	(-)%	τ_2/ps	%	τ_3/ps	%	τ_4
X_5	460	---	---	7	<0.2	93	1.6±0.1	---	---
	470	---	---	27	<0.2	7	2.0±0.1	---	---
	480	---	---	23	<0.2	77	2.5±0.1	---	---
	490	---	---	36	<0.2	64	3.0±0.3	---	---
X_4	500	---	---	34	0.30±0.11	66	3.2±0.2	---	---
	510	30	<0.2	29	0.48±0.08	41	4.0±0.1	---	---
	520	22	<0.2	34	0.72±0.09	44	5.0±0.2	---	---
$X_3(1P_{3/2}1P)$	530	12	<0.2	43	0.82±0.12	45	7.4±0.4	---	---
	540	4	<0.2	48	0.89±0.04	48	9.6±0.3	---	---
	550	3	<0.2	49	1.10±0.04	48	11.5±0.3	---	---
	560	4	<0.2	49	1.09±0.04	48	13.5±0.3	---	---
$X_2(2S_{3/2}1S)$	570	4	<0.2	49	1.01±0.03	46	13.7±0.4	1	ns
	580	4	<0.2	49	0.78±0.04	45	14.9±0.6	2	ns
	590	4	<0.2	48	0.66±0.05	42	17.1±1.2	6	ns
	600	5	<0.2	47	0.63±0.06	40	46.2±4.2	8	ns
$X_1(1S_{3/2}1S)$	610	4	<0.2	47	0.90±0.08	45	70.0±7.0	4	ns
	620	4	<0.2	47	0.81±0.07	45	46.8±3.6	4	ns
	630	4	<0.2	48	0.85±0.07	45	30.3±2.0	3	ns
	640	4	<0.2	48	0.83±0.07	48	21.8±1.0	---	---
TES	650	4	<0.2	47	0.78±0.10	49	13.0±0.6	---	---
	660	3	<0.2	48	1.36±0.48	49	7.1±0.5	---	---

Table S6. Complete set of fit parameters for D = 5.4 nm quantum dots PL up-conversion signals detected at different wavelengths. Notice the negative sign for the first and second terms.

State	λ/nm	(-)%	τ_1/ps	(-)%	τ_2/ps	%	τ_3/ps	%	τ_4
X_6	460	---	---	50	<0.2	50	1.8±0.1	---	---
	470	---	---	50	0.20±0.05	50	1.8±0.1	---	---
	480	---	---	30	0.20±0.10	70	2.0±0.1	---	---
X_5	490	---	---	50	0.21±0.03	50	2.4±0.1	---	---
	500	---	---	38	0.43±0.11	62	2.8±0.2	---	---
	510	---	---	54	0.33±0.04	46	2.9±0.2	---	---
X_4	520	---	---	54	0.51±0.05	46	3.7±0.2	---	---
	530	---	---	53	0.54±0.05	47	4.3±0.3	---	---
	540	---	---	52	0.54±0.06	48	4.8±0.3	---	---
$X_3(1P_{3/2}1P)$	550	4	<0.2	48	0.54±0.05	48	7.3±0.4	---	---
	560	4	<0.2	48	0.66±0.06	48	12.9±0.6	---	---
	570	4	<0.2	48	1.04±0.08	48	19.3±0.9	---	---
	580	4	<0.2	48	1.11±0.08	48	19.2±0.9	---	---
$X_2(2S_{3/2}1S)$	590	4	<0.2	48	0.92±0.08	48	20.1±1.0	---	---
	600	4	<0.2	48	0.91±0.07	48	20.8±1.0	---	---
	610	4	<0.2	47	0.73±0.08	43	15.0±1.0	6	ns
	620	5	<0.2	47	0.60±0.07	35	30.4±2.7	13	ns
$X_1(1S_{3/2}1S)$	630	5	<0.2	47	0.70±0.07	36	74.6±9.4	12	ns
	640	5	<0.2	46	0.68±0.09	42	75.9±9.0	7	ns
	650	5	<0.2	47	0.77±0.08	43	63.1±6.2	5	ns
	660	5	<0.2	46	0.58±0.09	49	42.7±1.8	---	---

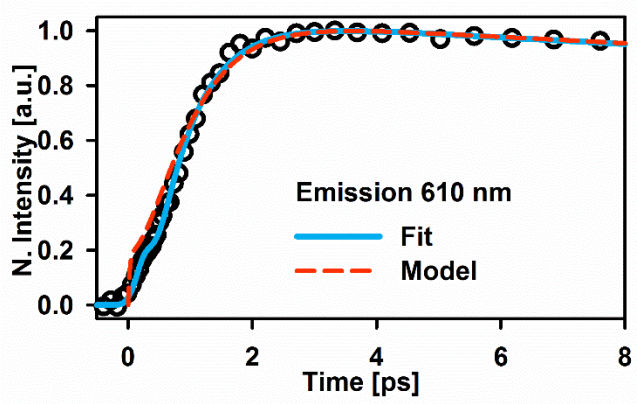

Figure S5. Photoluminescence up-conversion transient, fit and kinetic model for D = 4.4 nm quantum dots detected at 610 nm.

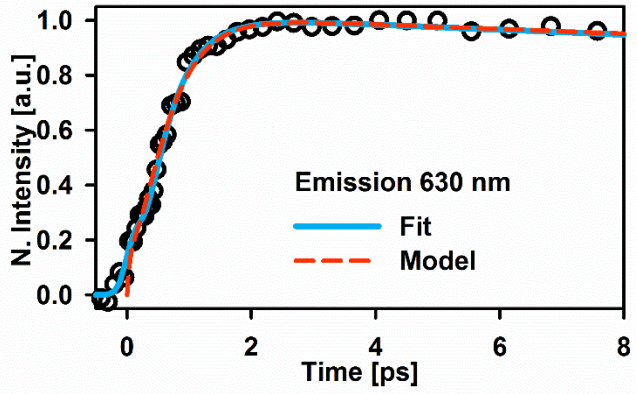

Figure S6. Photoluminescence up-conversion transient, fit and kinetic model for D = 5.4 nm quantum dots detected at 630 nm.

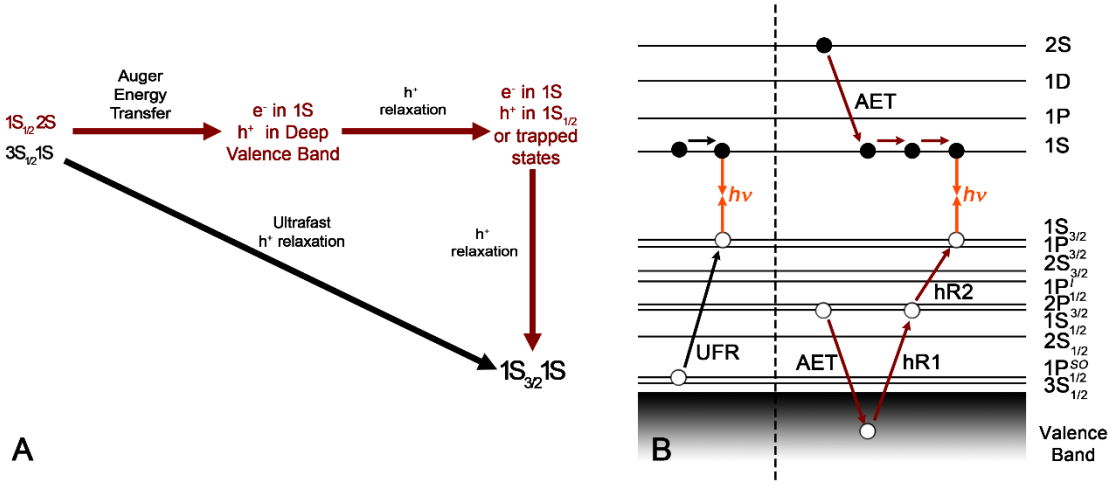

Figure S7. Kinetic deactivation pathways (A) proposed for the $X_1(1S_{3/2}1S)$ state yielding a slow accumulation channel (red arrows) in the band edge hole states after pumping with 400 nm (3.1 eV) pulses and an ultrafast (black arrow) accumulation. (B) Shows the same relaxation pathways in an energy level diagram.

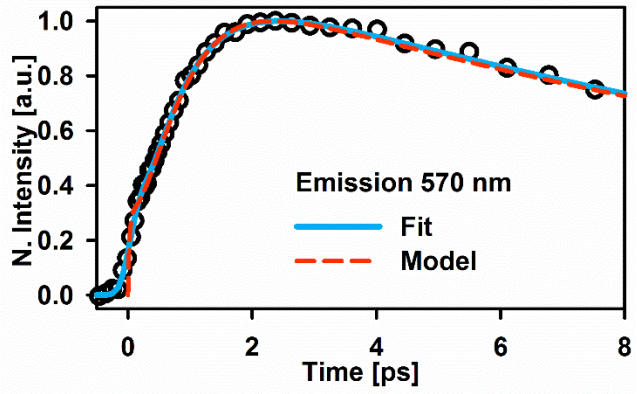

Figure S8. Photoluminescence up-conversion transient, fit and kinetic model for D = 4.4 nm quantum dots detected at 570 nm.

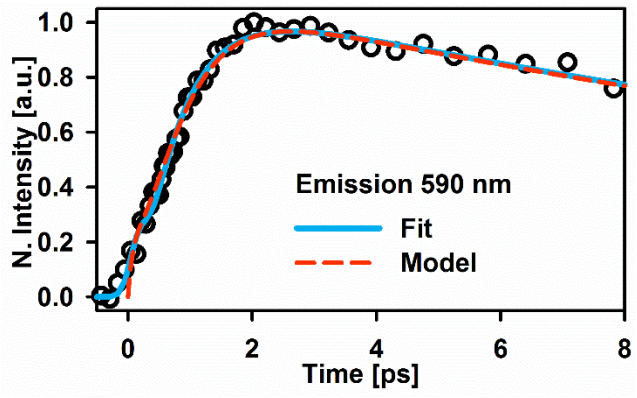

Figure S9. Photoluminescence up-conversion transient, fit and kinetic model for D = 5.4 nm quantum dots detected at 590 nm.

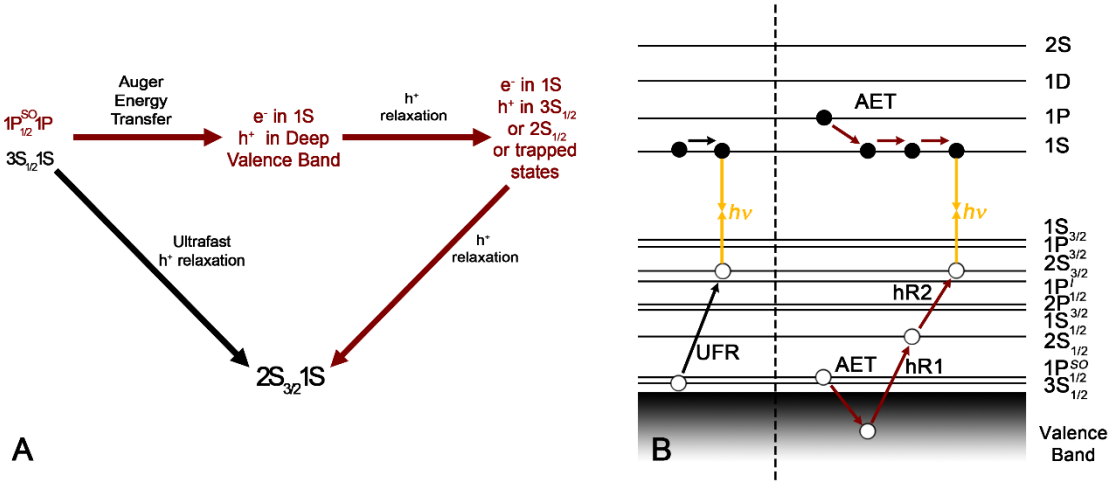

Figure S10. Kinetic deactivation pathways (A) proposed for the $X_2(2S_{3/2}1S)$ state yielding a slow accumulation channel (red arrows) in the band edge hole states after pumping with 400 nm (3.1 eV) pulses and an ultrafast (black arrow) accumulation. (B) Shows the same relaxation pathways in an energy level diagram.

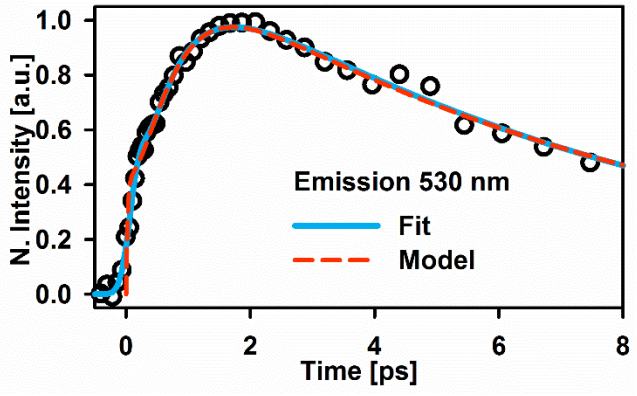

Figure S11. Photoluminescence up-conversion transient, fit and kinetic model for D = 4.4 nm quantum dots detected at 530 nm.

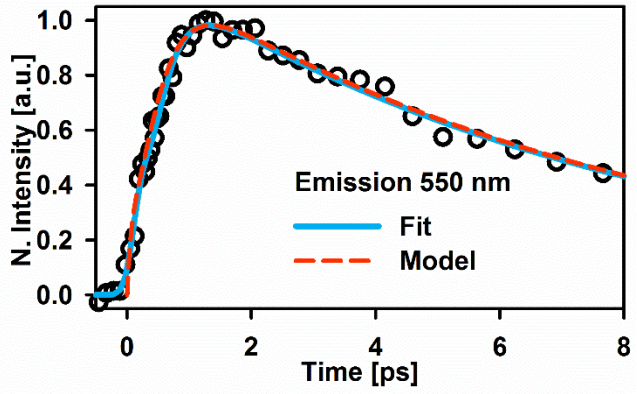

Figure S12. Photoluminescence up-conversion transient, fit and kinetic model for D = 5.4 nm quantum dots detected at 550 nm.

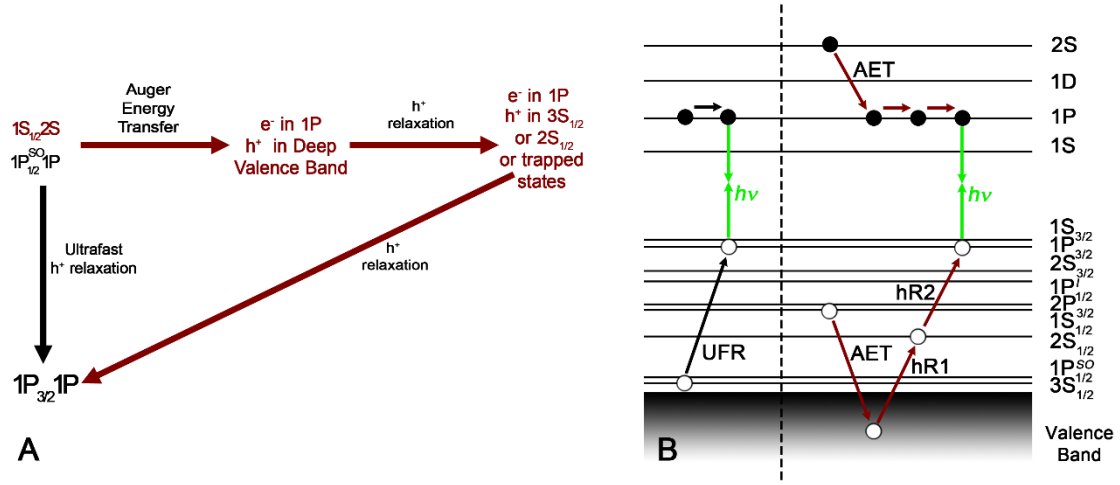

Figure S13. Kinetic deactivation pathways (A) proposed for the $X_3(1P_{3/2}1P)$ state yielding a slow accumulation channel (red arrows) in the band edge hole states after pumping with 400 nm (3.1 eV) pulses and an ultrafast (black arrow) accumulation. (B) Shows the same relaxation pathways in an energy level diagram.

Kinetic modelling details.

The kinetic schemes used to model the PL up-conversion transient data show that two parallel pathways are needed to form the final detected state indicated in each diagram. An ultrafast channel working in parallel with a stepwise process which involves three different steps. For the stepwise type process, two steps are required due to the Auger energy transfer from the electron to the hole and a subsequent fast hole relaxation from the deep valence band. The last step in the stepwise type process is related to the slower part of the accumulation of the signal.

All simulations were performed to qualitatively verify the behavior of the transient signals and the time constants are derived from those observed in the experiments. The models shown in the figures above only represent the accumulation of given states. As can be seen in Figures S7, S10 and S13, all three simulations follow a general scheme shown in Figure S14.

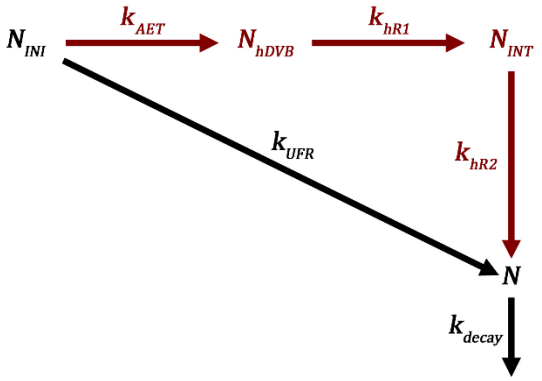

Figure S14. General population evolution pathways proposed for lower excitonic states $\boldsymbol{N}$ and the different intermediaries: "hole in deep valence state" $\boldsymbol{N_{hDVB}}$, and intermediary excitons or trapped states $\boldsymbol{N_{INT}}$, produced from the initially pumped states $\boldsymbol{N_{INI}}$ with 400 nm (3.1 eV) pulses.

The resulting population of the detected state $\boldsymbol{N}$ which can be one of the states $X_1(1S_{3/2}1S)$, $X_2(2S_{3/2}1S)$ or $X_3(1P_{3/2}1P)$, is overlapped with each one of the detected PL transient signals in Figures S5, S6, S8, S9, S11, and S12. The set of kinetic equations that are solved for each of the involved species are:

$$\frac{dN}{dt} = \boldsymbol{k_{UFR}N_{INI} + k_{hR2}N_{INT} - k_{decay}N} \quad \text{(Eq. S1)}$$

$$\frac{dN_{INT}}{dt} = \boldsymbol{-k_{hR2}N_{INT} + k_{hR1}N_{hDVB}} \quad \text{(Eq. S2)}$$

$$\frac{dN_{hDVB}}{dt} = \boldsymbol{-k_{hR1}N_{hDVB} + k_{AET}N_{INI}} \quad \text{(Eq. S3)}$$

$$\frac{dN_{INI}}{dt} = \boldsymbol{-(k_{AET} + k_{UFR})N_{INI}} \quad \text{(Eq. S4)}$$

where $\boldsymbol{k_{UFR}}$ is the associated constant of the ultrafast hole relaxation, $\boldsymbol{k_{AET}}$ is the electron to hole Auger Energy Transfer constant, $\boldsymbol{k_{hR1}}$ is the relaxation of the hole from the Deep Valence Band, $\boldsymbol{k_{hR2}}$ is the hole relaxation of the near Band-Edge states and $\boldsymbol{k_{decay}}$ is the total or net decay constant of the detected state that includes all relaxation processes of the detected signal. $\boldsymbol{N_{INI}}$ is the population of the complete set of the initially pumped states, $\boldsymbol{N_{INT}}$ is the population of the intermediaries near the Band-Edge and trapped states and, $\boldsymbol{N_{hDVB}}$ is the population of the states that involves the hole in a hot state deep in the valence band.

For a kinetic system where both a direct and a stepwise formation pathway are proposed (Scheme S14), the analytical solution of the time-dependent population of $\boldsymbol{N}$ is determined by a triexponential function and a constant (these solutions consider that the final decay of the lower excitons occur on a much longer time scale, that is, the well know slow last step approximation):

$$\boldsymbol{N_t = N_{INI_0} * \left\{1 - a_1 * e^{-(k_{AET}+k_{UFR})*t} + a_2 * e^{-k_{hR1}*t} - a_3 * e^{-k_{hR2}*t}\right\}} \qquad \text{(Eq. S5)}$$

where:

$$\boldsymbol{a_1 = \left[1 + \frac{k_{AET}}{k_{hR1} - k_{AET} - k_{UFR}} * \left(1 + \frac{k_{hR1}}{k_{hR2} - k_A - k_{UFR}}\right)\right]} \qquad \text{(Eq. S6)}$$

$$\boldsymbol{a_2 = \left[\frac{k_{AET}}{k_{hR1} - k_{AET} - k_{UFR}} * \left(1 + \frac{k_{hR1}}{k_{hR2} - k_{hR1}}\right)\right]} \qquad \text{(Eq. S7)}$$

$$\boldsymbol{a_3 = \left[\frac{k_{AET} * k_{hR1}}{k_{hR1} - k_{AET} - k_{UFR}} * \left(\frac{1}{k_{hR2} - k_{hR1}} - \frac{1}{k_{hR2} - k_{AET} - k_{UFR}}\right)\right]} \qquad \text{(Eq. S8)}$$

The kinetic system imposes the condition that k_A and k_{UFR} are at least an order higher than k_{hR1} and k_{hR2}. While evaluating the variations of k_{hR1} and k_{hR2}, the preexponential factors become:

$$\boldsymbol{k_{hR1} > k_{hR2}, \quad a_1 > 0 \quad a_2 > 0 \quad a_3 > 0} \qquad \text{(Eq. S9)}$$

$$\boldsymbol{k_{hR1} < k_{hR2}, \quad a_1 > 0 \quad a_2 < 0 \quad a_3 < 0} \qquad \text{(Eq. S10)}$$

Whichever condition implies that the formation of $\boldsymbol{N_t}$ will be composed by a two negative and one positive exponential functions. This kinetic scheme agrees with the transient signals detected for the simulated excitonic states.